The 2010 IEEE/RSJ International Conference on
Intelligent Robots and Systems
October 18-22, 2010, Taipei, Taiwan

Shared Autonomy System for Tracked Vehicles to Traverse Rough Terrain Based on Continuous Three-Dimensional Terrain Scanning

Yoshito Okada, Keiji Nagatani, Kazuya Yoshida, Tomoaki Yoshida and Eiji Koyanagi

***Abstract*— Tracked vehicles are frequently used as search-and-rescue robots for exploring disaster areas. To enhance their traversability on rough terrain, some are equipped with "active flippers." However, manual control of such flippers also increases the operator's workload, particularly for tele-operation with limited camera views.**

To eliminate this tradeoff, we developed a shared autonomy system using an autonomous controller for flippers that is based on continuous three-dimensional terrain scanning. In our system, real-time terrain slices near the robot are obtained using three laser range sensors, and these are integrated to generate three-dimensional terrain information. In this paper, we introduce the autonomous controller for the flippers and validate the reliability of the shared autonomy system through experimental results on actual rough terrain.

I. INTRODUCTION

Search-and-rescue robots [1] are being developed by a number of institutes for the purpose of exploring disaster areas and obtaining information on victims to support rescue operations and minimize the risks of secondary disasters to rescuers and victims. For these robots, high mobility on the rough terrain of disaster areas comprising rubble is extremely important, so tracked vehicles are mainly used [2][3].

To enhance the traversability and stability of tracked vehicles for search-and-rescue operations, some are equipped with swingable sub-tracks called "active flippers," which negotiate steps and bumps in hazardous environments. Our tracked vehicle testbed "Kenaf" (Fig. 1) contains four active flippers and has such high mobility that it won the best mobility award twice in the RoboCupRescue Real Robot League [4] in 2007 and 2009.

However, we observed that the use of active flippers also increases the workload of the operator controlling the robot. In particular, it becomes more difficult when the operator tele-operates the robot with limited camera views on the robot.

To eliminate this situation, we proposed a shared autonomy system using an autonomous controller for active flippers in 2009 [5]. In that paper [5], we reported on the previous system that was successfully incorporated into Kenaf and confirmed that the autonomous controller reduces the operator's workload and maintains a stable pose of the robot while traversing actual rough fields. The previous controller was based on real-time terrain slices along the flippers that are obtained by two laser range sensors attached to both sides of the robot. However, the previous controller could not generate flipper motions to negotiate forward narrow steps/bumps between the flippers on both sides because they were out of the scanning range for the laser range sensors.

This work was supported by Strategic Advanced Robot Technology, an R&D project of the NEDO, Japan.

Y. Okada, K. Nagatani and K. Yoshida are with Tohoku University, 6-6-01 Aramaki Aza Aoba, Aoba-ku, Sendai 980-8579, Japan, yoshito@astro.mech.tohoku.ac.jp

T. Yoshida and E. Koyanagi are with Chiba Insutitute of Technology

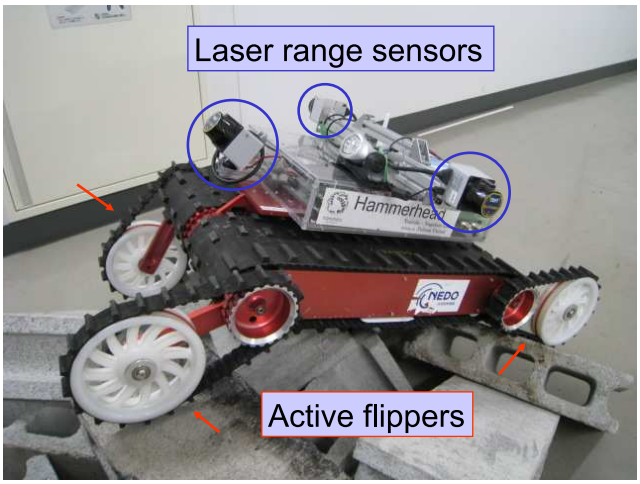

Fig. 1. Tracked vehicle testbed Kenaf

TABLE I
BASIC SPECIFICATIONS OF KENAF

Dimensions	W 400 [mm] × L 500 [mm]
Weight	20 [kg]
Length of flippers	235 [mm]
Degrees of freedom	6 (2 main tracks and 4 flippers)

In this paper, we introduce a new shared autonomy system to assist the operator of a tracked vehicle traversing rough terrain. The new system is derived from the previous one, and the new autonomous controller can generate flipper motions negotiating narrow steps/bumps between the flippers, which is an improvement on the previous system. Fig. 2 shows a comparison between the autonomous controllers for the flippers in the new and previous systems. The new controller applies three laser range sensors located at both sides and the front of the robot. The additional front laser range sensor obtains a slice of the shape of terrain being immediately traversed by the robot. Moreover, the new controller integrates the current three terrain slices from the three laser range sensors and various recent terrain slices from the front sensor on the basis of estimated positions and postures tagged to each slice, to estimate the three-dimensional shape of the terrain under the robot. Thus, the new controller can generate

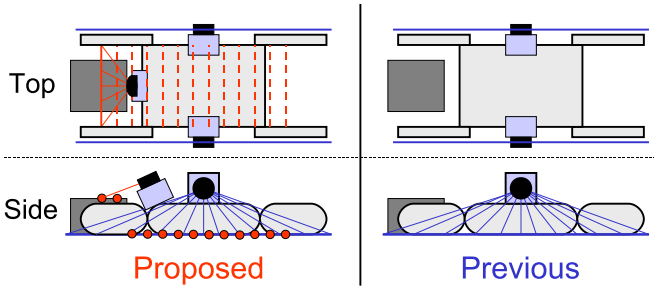

Fig. 2. Comparison between proposed controller and previous controller

better flipper motions for traversing rough terrain than the previous one, on the basis of richer information of the terrain shape.

There have been several studies on tracked vehicles to automatically traverse rough terrain using a controller/mechanical behavior.

ROBHAZ-DT3 [6] contains a passive joint between an anterior and posterior tracks; This joint adaptively rotates to enable good locomotion on rough terrain such as stairs.

HELIOS carrier [7] is equipped with a active tail-like mechanism; This tail is autonomously controlled on the basis of the attitude of the robot and distances to the ground. It assists the robot to move over stairs or steps.

An autonomous controller for active flippers has also been reported [8]; This controller determins the velocity of each flipper on the basis of the torque of each flipper and distances to the ground.

The rest of this paper is organized as follows. In Sec. II, we introduce our tracked vehicle testbed Kenaf in brief. In Sec. III, we describe our strategy for the autonomous control of flippers; this strategy is based on the motions of flippers tele-operated by expert operators as well as the strategy of the previous controller. In Sec. IV, we present an algorithm for realizing the strategy described in Sec. III by focusing on improved points from the algorithm of the previous controller. We then present our experiment; we applied the new shared autonomy system, including the new autonomous controller for the flippers to Kenaf and performed actual experiments in simulated disaster environments to confirm its advantages over the previous system and its validity. In Sec. V, we report our experiment results and discuss our findings. Finally, we present the conclusions of our study in Sec. VI.

II. Control Target

The new shared autonomy system was incorporated into the tracked vehicle testbed Kenaf (Fig. 1), which is the same as what was done in the previous study [5]. Kenaf is a 6-D.O.F (degree of freedom) tracked vehicle testbed for rescue operations; it has two main tracks covering the body and four active flippers, one located at each corner of the body.

Kenaf contains three laser range sensors on the front and both sides of the body to obtain real-time terrain slices. All motors of Kenaf are encoder-equipped, and the circumferential velocities of the main tracks and angular positions of the flippers are available. Kenaf contains a 3-D.O.F. gyroscope and a gravity sensor. Moreover, Kenaf has a three-dimensional odometry unit [9] that uses the outputs of the main tracks' encoders, the gyroscope, and the gravity sensor to estimate the position and posture of its body.

On rough terrain, it is quite difficult to estimate a position with high accuracy over long distances when using a dead-reckoning technique such as odometry. However, the proposed controller only needs reliable positions along short trajectories over the entire length of Kenaf that is approximately 90 [cm]. This is why we used position estimation based on three-dimensional odometry.

III. Control Strategy For Flippers

In this study, we aimed to achieve a smooth traversal of a tracked vehicle by a unskilled operator with our new shared autonomy system comprising a manual controller for main tracks and an autonomous controller for active flippers; the performance should be comparable to a skilled operator using a full-manual controller. Thus, similar to what was done in the previous study [5], we applied control strategies based on flipper motions operated by skilled operators to the new autonomous controller for the flippers. In the previous paper [5], we listed the following three features of full-manual operations by skilled operators:

- To enable the robot to traverse terrain smoothly, its posture must be maintained according to the slope of the ground surface.
- To enable good locomotion, the main tracks and the flippers should be in contact with the ground to the greatest extent possible.
- When the pose of the robot is unstable, rollover should be prevented by the motion of the flippers.

Taking the three above considerations into account, we applied the following strategy for the flippers and robot body:

1) The posture of the robot body must be maintained parallel to the least-squares plane of the ground surface, and the robot body must make contact with the ground.
2) The desired posture can be realized by changing the angular positions of the flippers.
3) The desired pose (desired posture and flipper positions) must be evaluated and redefined if it is unstable.

IV. Algorithm for Controller for Flippers

In this section, we present an algorithm based on the strategy described in Sec. III. The algorithm for the new controller is derived from that for the previous controller and consists of similar procedures. In the following subsections, we introduce improvements on the algorithm of the previous controller as well as the schema and each procedure of the new algorithm in detail.

A. Improved points upon the previous algorithm

The most significant improvement on the previous algorithm is the use of slices for the shape of the forward terrain being immediately traversed by the robot; these are

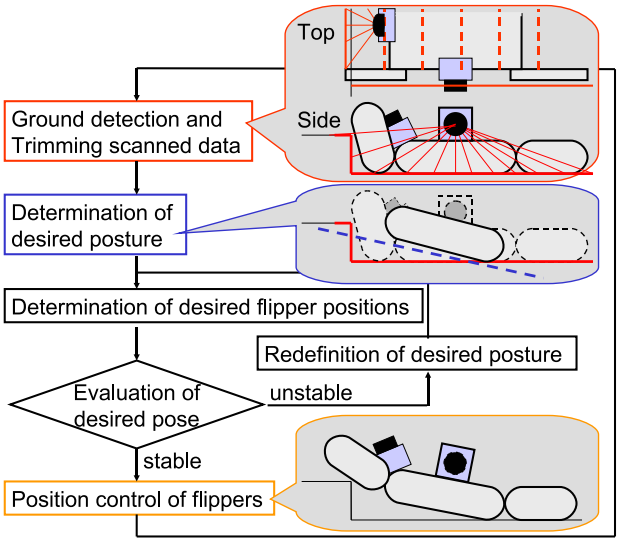

Fig. 3. Algorithm for autonomous control of flippers

obtained by the additional laser range sensor attached to the front of the robot body. The obtained terrain slices from the three laser range sensors are stored and tagged with the estimated position and posture of the robot body at the moment of each terrain scanning. These stored slices are integrated according to the procedure described in Sec. IV-D to generate three-dimensional information for the terrain under the robot, which is used in the procedure described in Sec. IV-E.

B. Schema of the new algorithm

Fig. 3 shows a schema of the algorithm for the new autonomous controller for flippers. The new control algorithm is divided into six procedures, which is the same as the previous algorithm. The new algorithm is summarized as given below.

(1) Slices of the shape of the terrain around the robot are first obtained from the three laser range sensors attached to the robot body and the three-dimensional terrain shape under the robot is estimated. (2) The desired posture of the body is then calculated on the basis of the estimated terrain surface. (3) the desired positions of the flippers that realize the desired posture of the body are also determined. Next, (4) the stability of the desired posture and flipper positions is evaluated. If the stability is not enough, (5) the desired pose is redefined and steps (3)-(5) are repeated. When the desired flipper positions that realize a stable posture are generated, (6) position control of the flippers is finally performed.

C. Coordinate systems

Let the robot coordinate system be right-handed, its origin be the center of the robot, its x-axis be orthogonal to the front face, and its z-axis be orthogonal to the top face. The position and posture of the robot can be represented by the relation between the global and robot coordinate systems.

In this study, we adopt the quaternion representation to describe positions and postures. For example, let the quaternion p denote the position vector $(x_{pos}, y_{pos}, z_{pos})^T$ in the global system and quaternion q denote the θ_{rot}-rotation about the axis of the unit vector $(x_{rot}, y_{rot}, z_{rot})^T$. The coordinate conversion from a local system $\{p, q\}$ to the global system can then be described by the following equation:

$$p_{global} = q \times p_{local} \times q^{-1} + p \quad (1)$$

$$p = [0, x_{pos}, y_{pos}, z_{pos}]^T \quad (2)$$

$$q = [\cos(\theta_{rot}/2), x_{rot}\sin(\theta_{rot}/2), y_{rot}\sin(\theta_{rot}/2), z_{rot}\sin(\theta_{rot}/2)]^T \quad (3)$$

D. Ground detection and trimming scanned data

The scanned points U in the robot coordinate system at the moment of scanning are first obtained by a laser range sensor on the robot. We tag U with the estimated position p and posture q in the global system at the moment of scanning and define them as the two-dimensional terrain information $S = \{U, p, q\}$. Let subscripts l, r, and f denote terrain slices from the left,right, and front sensors, respectively, and let subscript n indicate a terrain slice obtained during the nth control loop. We can now describe the two-dimensional terrain information obtained in the nth control loop as $S_{l,n}$, $S_{r,n}$, and $S_{f,n}$. In this loop, we use S_n to denote the union of $S_{l,n}$, $S_{r,n}$, $S_{f,n}$, and the terrain information from the front laser range sensor in recent loops as described by the following equation:

$$S_n = \{S_{l,n}, S_{r,n}, S_{f,m}, S_{f,m+1}, \ldots, S_{f,n}\} \quad (4)$$

$$m = \min\{i \in Z | \sum_{j=i}^{n-1} |p_{f,j+1} - p_{f,j}| < L_{threshold}\} \quad (5)$$

It should be noted that we only apply forward terrain information obtained during the last $L_{threshold}$-length trajectory to take into account accumulative errors for the position estimation.

Scanned points to be targeted in the following procedures are then selected out of S_n. If the desired pose determined in a following procedure is realized by Δt later, the robot position p' after Δt can be described by the following equation:

$$p' = p_{cur} + q_{cur} \times [0, V_{cur}\Delta t, 0, 0]^T \times q_{cur}^{-1} \quad (6)$$

where V is the translational velocity of the robot and the subscript "cur" denotes a current value. We trim the scanned points in S_n based on p' through the following steps. A coordinate conversion of a scanned point u from the tagged system $\{p, q\}$ to the robot system $\{p', q_{cur}\}$ is described by the following equation:

$$u' = q_{cur}^{-1} \times (q \times u \times q^{-1} + p - p') \times q_{cur} \quad (7)$$

We apply this conversion to each $S = \{U, p, q\} \in S_n$ and generate the three-dimensional terrain information U'_n, in which scanned points are represented in the same coordinate system.

$$U'_n = \{U'_{l,n}, U'_{r,n}, U'_{f,m}, U'_{f,m+1}, \ldots, U'_{f,n}\} \quad (8)$$

We then select the target points U_{target} for the following procedures out of U'_n according the following equation:

$$U_{target} = \{u \in U'_n | \quad -L_{max}/2 \leq x \leq L_{max}/2 \\ and \ -W/2 \leq y \leq W/2 \quad \} \ (9)$$

where L_{max} is the entire length of the robot, including the length of a flipper, and W is the width of the robot.

E. Determination of desired posture

Although this and the following procedures are based on U_{target} including terrain information from the additional front sensor, they are similar to the procedures of the previous algorithm [5]. Hence, we do not go into their details and only introduce the essentials.

As mentioned previously, for the control strategy for the new controller, the desired posture of the robot body is initialized to be parallel to the least-squares plane of the ground surface and in contact with the ground. We first calculate the quaternion q_{target} which represents the parallel posture of the least-squares plane of U_{target} determined in the last subsection. U_{target} is then converted to the robot system for the case where the posture of the robot is equal to q_{target}; let this be U'_{target}. Finally, we convert U'_{target} to the robot system for the case where the robot makes contact with the ground; let this be U''_{target}. The above conversions are summarized in the following equations using $u \in U_{target}, u' \in U'_{target}$ and $u'' \in U''_{target}$:

$$u' = q_{target} \times u \times q_{target}^{-1} \quad (10)$$

$$u'' = u' - [0, 0, 0, \max(z' \in U'_{target})]^T \quad (11)$$

To realize control strategy (1), we assume the converted terrain information U''_{target} as the target of following procedures.

F. Determination of desired positions of flippers

Next, we determine the desired positions of the flippers that realize the desired posture. To generate the desired flipper positions, we consider the flipper positions that make contact with the ground surface as represented by the three-dimensional terrain information U''_{target} in the desired robot system.

In particular, we determine if each flipper can make contact with each scanned point $u'' \in (\{U''_{l,n}, U''_{r,n}\} \cap U''_{target})$— one of the scanned points obtained by the left or right laser range sensor— and calculate the contact angular position of the flipper when contact can be made. The desired position of each flipper is determined for the maximum angular position of the flipper.

Because the shape of Keanf's flippers comprises straight and round sections, we distinguish whether every scanned point makes contact at a straight or round section and use the appropriate geometric calculation to realize strategy (2).

G. Stability evaluation of desired pose

We have obtained the desired pose (posture of the robot body and positions of the flippers). In this procedure, we evaluate its stability on the basis of the normalized energy stability margin (NESM) [10] proposed by Hirose et al. as well as the previous algorithm.

The NESM is a criterion used to evaluate the stability of a robot based on the vertical distance between the initial position of the center of gravity and its highest position when tumbling around an axis through two contact points between the robot and the ground. Although it is mainly used for walking robots, there is no conceptual difference when applying this criterion to the case of tracked vehicles with flippers.

In the new algorithm, four contact points of Kenaf in the desired posture are calculated in the procedure described in Sec. IV-F. We assume four tumbling axes that pass through the contact points on the front right and front left, front right and rear right, front left and rear left, and rear right and rear left. The stability of Kenaf is determined by the minimum value of the NESM about these four axes.

H. Redefinition of desired pose

When the stability of the desired pose calculated in the procedure described in the last subsection is less than a predetermined threshold, we redefine the desired posture and flipper positions as well as the previous algorithm according to strategy (3). We divide this procedure into the following steps:

1a. When the NESM about the front or rear is adopted, reduce the pitch angle of the desired posture to close to zero.
1b. When the NESM about the right or left is adopted, reduce the roll angle of the desired posture to close to zero.
2. Redefine the desired flipper positions by recalculating them to realize the redefined desired posture.
3. Evaluate the NESM about the redefined posture and flipper positions.

We repeat the above routine until a desired stable pose is generated.

I. Position control of flippers

To realize a desired stable posture of the robot body determined through the abovementioned procedures, we finally perform position control of the flippers. In the new algorithm, we adopt the conventional PID controller. In addition, to realize the desired angular positions of the flippers θ_{ref} by Δt assumed in Sec. IV-D, we determine each maximum angular velocity of the flippers ω_{max} using the following equation:

$$\omega_{max} = C \frac{|\theta_{cur} - \theta_{ref}|}{\Delta t} \quad (12)$$

where θ_{cur} is the current angular positions of the flipper and C is a given constant of proportionality.

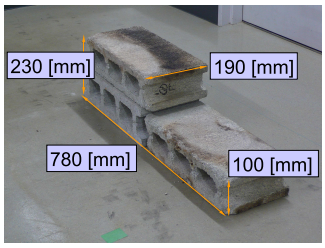

Fig. 4. Bump comprising concrete blocks

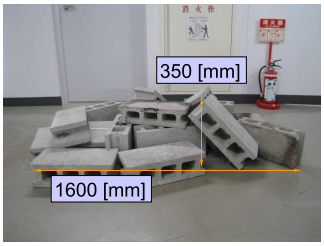

Fig. 5. Complex field comprising randomly positioned concrete blocks

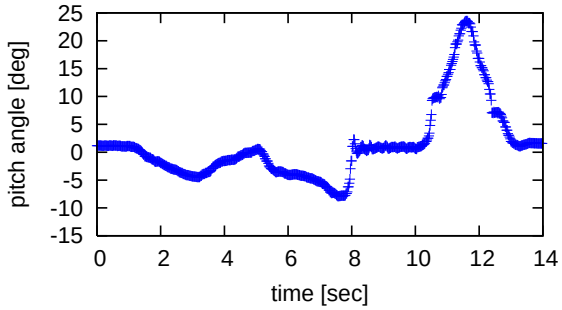

Fig. 6. Change in pitch angle on bump

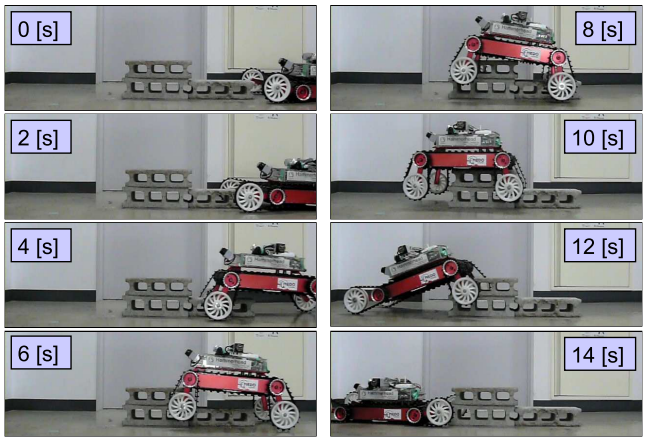

Fig. 7. Snapshots of Kenaf while traversing bump

V. Experiments

A. Overview

We incorporated the new shared autonomy system, including the autonomous controller described in Sec. IV, into Kenaf and performed experiments on two rough fields comprising concrete blocks to validate the new system. We set up a narrow bump (Fig. 4) and complex field to simulate disaster areas for the experimental fields and compared traversals using the new system and another system on each field. In addition, we obtained the changes in posture of Kenaf using the built-in 3-D.O.F gyroscope for every traversal and compared them.

For every traversal, we assumed that the range $L_{threshold}$ of integration of the terrain information back to the recent trajectory to be 100 [cm], the time delay Δt until realization of the desired pose to be 0.5 [sec], the threshold of the NESM to be 10 [cm] of half NESM on level ground, and the given constant of proportionality C for the maximum angular velocity of the flippers to be 1.3.

B. Comparative experiment with previous system

1) Overview: First a comparative experiment with the previous system [5] was performed on a narrower bump than the width of Kenaf and comprising three concrete blocks (Fig. 4). We operated the main tracks of Kenaf manually and the flippers autonomously using each autonomous controller and made Kenaf interact with the short side of the bump to observe whether or not Kenaf was assisted by the autonomous controller for the flippers to traverse the bump.

2) Results and discussions: Fig. 6 shows the change in the pitch angles of Kenaf's body during traversal when using the new shared autonomy system, and Fig. 7 shows snapshots. The graph and snapshots indicate that the flipper motions generated by the autonomous controller in the new system maintained a stable posture of Kenaf, maintained contact with the surface of the bump during traversal and made Kenaf traverse along the entire length of the bump.

In constant, for the previous system using laser range sensors on both sides, its autonomous controller for the flippers could not detect the bump located out of the scanning planes, and Kenaf could not get over the bump. Because the bump could not be detected by the previous system, the previous system did not generate swinging-down motions of the front flippers to lift up the body over the top face of the bump, in contrast to the new system.

These results are typical and indicate the advantage of the new system using the additional laser range sensor at the front of the robot over the previous one.

C. Comparative experiment with an expert operator

1) Overview: Second, a comparative experiment was performed with manual control of the flippers by an expert operator on a complex field comprising twenty concrete blocks (Fig. 5) to simulate the terrain of a disaster area. To normalize the trial conditions, we set the circumferential velocities of the main tracks to be 10 [cm/s] on each trial; the expert operator only controlled the flippers manually in the comparative case.

2) Results and discussions: Figs. 8 and 9 show the change in pitch angle and roll angle, respectively, of Kenaf's body, and Fig. 10 shows snapshots of the traversal when using the new shared autonomy system. The elapsed times were 22 [sec] with the new system and 23 [sec] with the full-manual control by an expert operator. For comparison purposes, the horizontal axes in Figs. 8 and 9 indicate the ratios obtained by dividing the elapsed times by the total time required to traverse the field.

As Fig. 10 indicates, the new shared autonomy system also realized a stable traversal even on a complex field. Moreover, from Figs. 8 and 9, we can see that the behaviors of the posture for Kenaf's body during the traversals due to the autonomous/manual motions of the flippers were quite similar. In particular, for the pitch angles, the new system kept the attitude of Kenaf's body lower along the entire length of the trajectory. However, we note that the stability

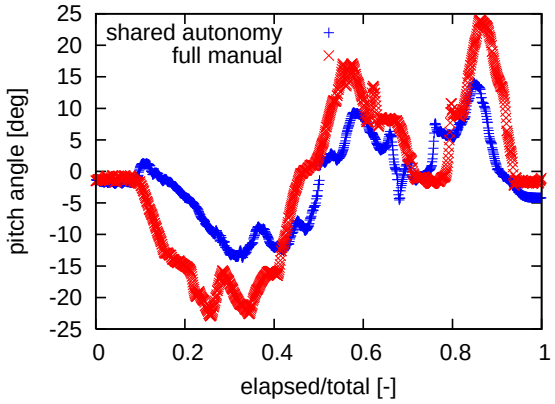

Fig. 8. Change in pitch angle on complex field

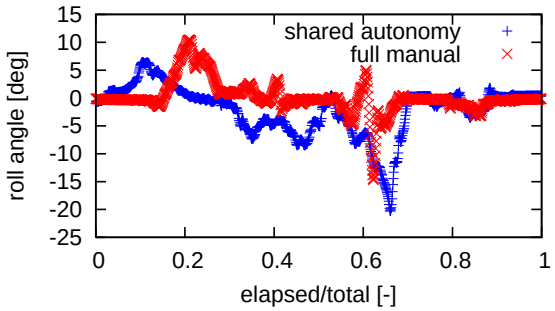

Fig. 9. Change in roll angle on complex field

of Kenaf is more likely to depend on the pitch angle than roll angle because the entire length of Kenaf, including the length of a flipper, is about twice as much as its width. Nevertheless, we can say that the traversal with the new system is as stable as that with manual control of the flippers by an expert operator.

From these results, we confirmed the validity of the control strategy derived on the basis of flipper motions operated by expert operators and the reliability of the control algorithm realizing the strategy.

VI. Conclusions

In this study, we constructed a shared autonomy system for tracked vehicles with active flippers; the system comprised a manual controller for the main tracks and an autonomous controller for flippers. It is based on continuous terrain scanning using three laser range sensors. The obtained terrain shapes are integrated on the basis of the estimated positions and postures of the robot tagged with each shape and are used for autonomous control of the flippers. The algorithm for the autonomous controller for flippers is based on the control strategy derived from flipper motions performed through manual control by an expert operator. It generates flipper motions that control the posture of the body of a robot according to the average attitude above the ground surface unless the robot has enough stability on rough terrain.

We carried out actual experiments in several fields using our testbed and implemented the proposed shared autonomy system. The results showed that the proposed system achieves a stable traversal that is as smooth as full-manual operation, including manual control of the flippers by an expert operator, when the operator only specifies a desired direction to the robot.

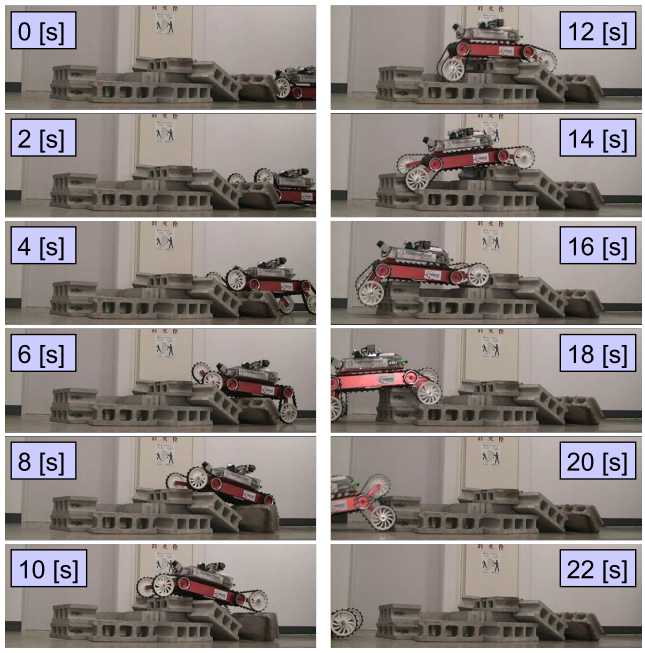

Fig. 10. Snapshots of Kenaf while traversing complex field

References

[1] S. Tadokoro, F. Matsuno and A. Jacoff, “Special Issues on Rescue Robotics”, Advanced Robotics Vol.19 No.3, No.8, 2004

[2] H. Miyanaka, N. Wada, T. Kamegawa, N. Sato, S. Tsukui, H. Igarashi and F. Matsuno, “Development of an unit type robot “KOHGA2” with stuck avoidance ability”, *The IEEE International Conference on Robotics and Automation*, 2007, pp. 3877–3882

[3] Y. Tanaka, M. Arai, S. Hirose and S. Tsukui, “Development of “Souryu-V” with Mono-Tread-Crawlers and Elastic-Rods Joint”, *The IEEE International Workshop on Safety, Security, and Rescue Robotics*, 2006

[4] A. Jacoff, E. Messina, B.A. Weiss, S. Tadokoro and Y. Nakagawa, “Test Arenas and Performance Metrics for Urban Search and Rescue Robots”, *The IEEE/RSJ International Conference on Intelligent Robots and Systems*, 2003, pp. 3396–3403

[5] Y. Okada, K. Nagatani and K. Yoshida, “Semi-Autonomous Operation of Tracked Vehicles on Rough Terrain using Autonomous Control of Active Flippers”, *The IEEE/RSJ International Conference on Intelligent Robots and Systems*, 2009

[6] M. Kim, W. Lee and S. Kang, “Robhazdt3: Teleoperated Mobile Platform with Passively Adaptive Double-Track for Hazardous Environment Applications,” *The IEEE/RSJ International Conference on Intelligent Robots and Systems*, 2004, pp. 33–38

[7] M. Guarnieri, P. Debenest, T. Inoh, K. Takita, H. Masuda, R. Kurazume, E. Fukushima and S. Hirose, “HELIOS Carrier: Tail-like Mechanism and Control Algorithm for Stable Motion in Unknown Environments,” *The IEEE International Conference on Robotics and Automation*,2009

[8] K. Ohno, S. Morimura, S. Tadokoro, E. Koyanagi and T. Yoshida, “Semi-autonomous Control System of Rescue Crawler Robot Having Flippers for Getting Over Unknown-steps,” *The IEEE/RSJ International Conference on Intelligent Robots and Systems*, 2007, pp. 3012–3018

[9] K. Nagatani, N. Tokunaga, Y. Okada and K. Yoshida, “ Continuous Acquisition of Three-Dimensional Environment Information for Tracked Vehicles on Uneven Terrain”, *The IEEE International Workshop on Safety, Security, and Rescue Robotics*, 2008, pp.25–30

[10] S. Hirose, H. Tsukagoshi and K. Yoneda, “Normalized Energy Stability Margin: Generalized Stability Criterion for Walking Vehicles”, *The International Conference on Climbing and Walking Robots*, 1998, pp.71–76